

Lorentz Violation and Topologically Trapped Charge Carriers in 2D Materials

R. A. C. Correa¹, W. de Paula¹, A. de Souza Dutra², T. Frederico¹

¹ *Instituto Tecnológico de Aeronáutica, DCTA, 12228-900, São José dos Campos, SP, Brazil*

² *DFQ, Universidade Estadual Paulista-UNESP, 12516-410, Guaratinguetá, SP, Brazil*

The full spectrum of two-dimensional fermion states in a scalar soliton trap with a Lorentz breaking background is investigated in the context of the novel 2D materials, where the Lorentz symmetry should not be strictly valid. The field theoretical model with Lorentz breaking terms represents Dirac electrons in one valley and in a scalar field background. The Lorentz violation comes from the difference between the Dirac electron and scalar mode velocities, which should be expected when modelling the electronic and lattice excitations in 2D materials. We extend the analytical methods developed in the context of 1+1 field theories to explore the effect of the Lorentz symmetry breaking in the charge carrier density of 2D materials in the presence of a domain wall with a kink profile. The width and the depth of the trapping potential from the kink is controlled by the Lorentz violating term, which is reflected analytically in the band structure and properties of the trapped states. Our findings enlarge previous studies of the edge states obtained with domain wall and in strained graphene nanoribbon in a chiral gauge theory.

PACS numbers:

I. INTRODUCTION

Since the seminal work by Skyrme¹, where the first three-dimensional topological defect solution arising from a nonlinear field theory was presented in the context of particle physics, a very large number of studies reporting the impact of some kind of topological defect has appeared in the physics literature and, in recent years, this area of research remains one of the most active fields in many areas of the physics, including condensed matter physics², field theory³, and cosmology⁴. For instance, in an astrophysical scenario, topological defects arise largely from grand unified theories (GUTs) of elementary particles. In this case, it is expected that the known local gauge symmetry group $SU_C(3) \times SU_L(2) \times U_Y(1)$ resulted from an underlying symmetry group G after a series of spontaneous symmetry breakings. Thus, the early universe has gone through a number of phase transitions, with one or more several types of topological defects possibly being left behind.

Another interesting background, where we can find topological configurations, is high energy physics⁵. In this context, topological structures are found for example in the massive Thirring model⁶, in nonlinear chiral theories⁷, in the Gross-Neveu model⁸, in a chiral $SU(3) \times SU(3)$ model⁹, in an artificial spin-ice lattice¹⁰, and where the Peccei-Quinn symmetry is broken after inflation¹¹.

Nowadays we know that the carbon is the key ingredient in the called organic chemistry. From the viewpoint of condensed matter physics, the carbon plays a crucial role in the formation of new classes of topological materials¹² with a large variety of physical properties^{13,14}. In particular, the material named in the literature as graphene is the most famous due to their great potential for technological applications. Those materials are a two-dimensional (2D) allotrope of carbon, which consists of a monotonic layer of carbon atoms on a

honeycomb lattice. Its abundant electronic properties was studied for the first time using the tight-binding approximation¹⁵, where the structure of the electronic energy bands and Brillouin zones for graphite has been calculated. Although it is a nonrelativistic system, because the fermions move with a speed v_F , which is 300 times smaller than the speed of light c , the most remarkable feature of the graphene is that electronic properties can be described by the relativistic Dirac equation, as initially pointed by Semenoff¹⁶. Thus, we can use the well-established methods of quantum field theory in order to study the physics and topological properties of the graphene^{17,18}.

A special point of interest in graphene are the topological excitations, which are a direct consequence of its strong chemical bonding¹⁹ responsible for assuring a stability in the geometrical properties of the underlying lattice. Topological defects in graphene can lead to the appearance of an effective gauge field, which can be induced by wrinkles or ripples in its structures²⁰, when the graphene sheet is under tension²¹, and by displacements along bond directions²².

Topological excitations of the 2D lattice have its counterpart in the electronic properties of the material. One example, is the Jackiw-Pi theory that predicts a Dirac zero mode, associated with vortex solutions of the gauge field coupled to the electrons, leading to charge fractionalization^{23,24}. The Jackiw-Pi theory was further generalized to non-chiral models^{25,26}, where the implications of different gauge groups in the gap formation, considering scalar, vector, and fermion excitations were studied. In addition the finite-energy vortex solutions of the gauge models having the flux of the electromagnetic fields quantized leads to the Bohm-Aharonov effect even in the absence of external electromagnetic field. Furthermore, we can find an interesting supersymmetric model for graphene in Refs.^{27,28}.

Another example, of interest, is the possibility of soli-

tonic excitations in the 2D lattice from the nonlinear solutions of the field equations in nanoribbons (see e.g.²⁹). The static deformation of the scalar field forming a domain wall in a graphene layer has been analyzed in³⁰, where it was discovered an electronic domain wall spectrum associated with localized electronic states transverse to the wall, and propagating only in one dimension. They studied gapped graphene and found three confined states, one the zero-mode and one in the conducting and valence band. In strained graphene nanoribbon it was also studied a soliton trap which has electronic states confined to the wall associated with a Dirac zero mode solution in the trap³¹.

The topological confinement of electrons in bilayer graphene was proposed in³², where also the associated spectrum was computed numerically (for a recent review on the electronic properties of bilayer graphene see³³). Such theoretical proposal was experimentally verified by observing the valley transport properties at the bilayer graphene domain wall³⁴, and quite recently³⁵ it was possible to control these one-dimensional conducting channels in a gapped set up. The imaging of the confined states was done in³⁶ by using scanning tunnelling microscopic, and it was found that the associated conducting channels are mainly located close to the two edges of the domain wall.

We should remind that Jackiw and Rebbi³⁷ in 1976 proposed that Fermions can couple to bosonic soliton configurations in non-linear theories in (1+1) dimensions. In that work, it was concluded that there is a zero-energy bound state, where the solitons are degenerate doublets with fermion number $\pm 1/2$. Following this seminal paper, several works have been done with theories involving fermionic fields coupled to topological defects, such studies have included fermions and vortex solutions in abelian and nonabelian gauge theories³⁸, monopoles³⁹, supersymmetric field theories⁴⁰, condensed matter and relativistic field theories⁴¹, nanorings⁴², dense quark matter⁴³, Aharonov-Bohm and Aharonov-Casher problems⁴⁴, and topological superconductors⁴⁵.

Motivated by the work of Ref.³⁷, Chu and Vachaspati⁴⁶ obtained the full spectrum of fermion bound states on a scalar Z_2 kink in (1+1) dimensions. Indeed, a decade before in⁴⁷, it was speculated that the presence of possible fermionic bound states would inhibit the decay of cosmic strings. The method developed in Ref.⁴⁶ to solve the Dirac equation on a kink background has been shown to be extremely powerful. It enables to obtain analytically the bound state solutions. Later on, Dutra and Correa⁴⁸ have extended such method to study fermion bound-states and zero modes in the background of kinks within models presenting a structure with a false and a true vacuum. The spectrum of fermion bound-states of a class of asymmetrical scalar field potentials was analytically obtained in that work. Therefore, the findings of^{46,48}, in one-dimensional theory, suggest that a domain wall, or a soliton trap for electrons in 2D materials, should also presents an analytical representation of

the rich spectrum and the corresponding states adding this feature to the previous finding of³⁰ and³¹.

In the present work we generalize the analytical methods developed in⁴⁶ for field theories of fermions coupled to scalar kinks in (1+1) to (2+1) dimensions in order to obtain the electronic spectrum in the presence of such topological defect. We found analytically the excited states trapped by this domain wall, adding those to the ones previously obtained by³⁰ and³¹. Furthermore, we will explore the properties of the spectrum under the influence of constant external fields coupled to the fermions and also the associated impact due to the change of the kinetic term of the scalar field, which is given by Lorentz symmetry violation terms in the Lagrangian. Our motivation is to check the robustness of the electron spectrum when the properties of scalar field associated with modes of the 2D lattice are modified, in particular with respect to the propagation speed.

In fact, in a pioneer work, Kostelecky and Samuel⁴⁹ proposed Lorentz Symmetry Violation (LSV) in string theories, that was explored in several other physical scenarios (see e.g.⁵⁰ and references therein). In particular, some works have explored topological defects in the presence of LSV. For instance, we can find investigations using monopole and vortices^{51–56}, in a gauged $O(3)$ sigma model⁵⁷, on topological defects generated by two real scalar fields^{58–60}, in the propagation of electromagnetic waves⁶¹, and in traveling solitons systems^{62,63}.

This paper is organized as follows: in Section II we present the theoretical framework of the SME which is going to be analyzed and we find the classical field configurations associated to it. In Section III we compute the full spectrum of two-dimensional fermion states. In Section IV we present our conclusions and final remarks.

II. EXTENDED LAGRANGIAN WITH LORENTZ-VIOLATING INTERACTION

In this section, we will show the general form of the relativistic Lagrangian for a free spin-1/2 Dirac fermion ψ of mass m in the so-called standard-model extension. At this point it is important to remark that this theory is based on the idea of spontaneous Lorentz breaking in an underlying theory and has been used for various investigations placing constraints on possible violations of Lorentz symmetry, several of which depend crucially on the nonrelativistic physics of free massive fermions.

Our development is a generalization of the work⁴⁶, where it was studied the kink-fermion coupling in 1 + 1 dimension without Lorentz breaking. We extend the 1+1 theory studied in⁴⁶ to 2 + 1 dimensions including Lorentz breaking terms in the model in order to study the electronic properties of 2D materials in the presence of a kink. The extended Lagrangian density, adopted in the

present work, has the following form:

$$\mathcal{L} = \frac{1}{2} \partial_\mu \phi \partial^\mu \phi + k^{\mu\nu} \partial_\mu \phi \partial_\nu \phi - V(\phi) + i\bar{\psi} \gamma^\mu \overleftrightarrow{\partial}_\mu \psi - a_\mu \bar{\psi} \gamma^\mu \psi - i b_\mu \bar{\psi} \gamma_5 \gamma^\mu \psi - g \phi \bar{\psi} \psi, \quad (1)$$

where $A \overleftrightarrow{\partial}_\mu B \equiv A \partial_\mu B - (\partial_\mu A) B$, ϕ is a real scalar field, ψ is a two-component spinor, $V(\phi)$ is the potential, given in terms of a real scalar field, defining the bosonic sector of the specific model under analysis, g is the corresponding Yukawa coupling, $k^{\mu\nu}$ is a dimensionless coefficient for Lorentz violation that preserves *CPT*. It can be taken as real, symmetric, and traceless. The polarization tensor $k^{\mu\nu}$ in the context of 2D materials, represents the change in the scalar mode propagation with the direction, and its speed can be different from the electron Fermi velocity.

Furthermore, the quantities a_μ and b_μ are parameters that control the extent of Lorentz and *CPT* violation in the theory. At this point, it is important to remark that, in the context of the standard-model and quantum electrodynamics (QED) extensions, these parameters are determined by expectation values of Lorentz tensors arising from spontaneous Lorentz breaking in a more fundamental theory. Finally, in the above Lagrangian density, the γ^μ are the Dirac matrices, which in this work will be written as

$$\gamma^0 = \sigma^3 = \begin{bmatrix} 1 & 0 \\ 0 & -1 \end{bmatrix}, \quad \gamma^1 = i\sigma^1 = i \begin{bmatrix} 0 & 1 \\ 1 & 0 \end{bmatrix}, \quad (2)$$

$$\gamma^2 = i\sigma^2 = \begin{bmatrix} 0 & 1 \\ -1 & 0 \end{bmatrix}. \quad (3)$$

In order to justify the choice of such matrix representation, we point out that some years ago, these description has enabled to obtain the spectrum of fermion bound-states on the background of kinks of a class of asymmetrical scalar field potentials⁴⁸. In that work, such matrix structure allowed to find analytically the fermion configurations which has important consequences for cosmological and condensed matter systems. Another important matrix that will be useful is the γ_5 . In this context, its representation is given by

$$i\gamma_5 = -i\gamma^0\gamma^1\gamma^2 = - \begin{bmatrix} 1 & 0 \\ 0 & 1 \end{bmatrix}. \quad (4)$$

Note that for the bidimensional irreducible representation of the spinor space, the pseudovector and vector Lorentz breaking terms in the Lagrangian are the same, as the rotation of 180° in the plane is equivalent to the parity transformation, and mathematically the algebra is closed with the identity and the three Pauli matrices. Assuming isotropy for the given frame, namely $\vec{a} = \vec{b} = 0$, the net effect of the corresponding Lagrangian terms, produce only a trivial shift the Dirac spectrum and from now on we set $a_0 = b_0 = 0$.

Here, we would like to emphasize that, as expected, the gamma-matrices Eq. (2) and Eq. (4) satisfy the usual Clifford algebra

$$\{\gamma^\mu, \gamma^\nu\} = \gamma^\mu \gamma^\nu + \gamma^\nu \gamma^\mu = 2g^{\mu\nu}, \quad (5)$$

In this work, as an illustrative example, we choose the ϕ^4 theory^{64,65} which is given by a symmetric double-well potential

$$V(\phi) = \frac{\lambda}{4} (\phi^2 - \eta^2)^2, \quad (6)$$

where λ and η are real parameters. As we can see, this double-well potential has two minima, at $\phi = \pm\eta$. Moreover, there is reflectional symmetry since $V(\phi) = V(-\phi)$ and the vacuum manifold has two-fold degeneracy. At this point, it is important to remember that, in this model, the vacuum has an expectation value $\langle \phi \rangle = \pm\eta$. Therefore, in such a vacuum, the elementary fermion will have a mass $m_f = |g \langle \phi \rangle| = g\eta$, where we are taking $g > 0$ and $\langle \phi \rangle = \eta$. On the other hand, the mass associated to the scalar sector is $m_s = \sqrt{2\lambda}\eta$.

As we are studying a theory in $2+1$ dimensions, the tensor $k^{\mu\nu}$ in Eq. (1) is represented by a 3×3 matrix written in the form

$$k^{\mu\nu} = \begin{pmatrix} k^{00} & k^{01} & k^{02} \\ k^{10} & k^{11} & k^{12} \\ k^{20} & k^{21} & k^{22} \end{pmatrix}. \quad (7)$$

It is important to remark that the above matrix has arbitrary elements. However, if this matrix is real, symmetric, and traceless, the *CPT* symmetry is kept. Recently, a great number of works using a similar process to break the Lorentz symmetry, with a tensor like $k^{\mu\nu}$, have been used in the literature, from microscope⁶¹ to cosmological scales^{63,66-68}.

From the Lagrangian density (1), the Euler-Lagrange equation for ϕ is

$$\partial_\mu \partial^\mu \phi + k^{\mu\nu} \partial_\mu \partial_\nu \phi + V_\phi(\phi) = 0, \quad (8)$$

where $V_\phi(\phi) = dV(\phi)/d\phi$. Note that, in the above equations we are assuming that the back reaction due to the Yukawa coupling between the Dirac field and the scalar one can be neglected^{69,70}, in other words, the scalar field behaves like a classical background field⁷¹.

As we are interested in static solutions, where the field ϕ has dependence only in z , namely $\phi = \phi(z)$. Thus, the above equation becomes

$$\partial_z^2 \phi = \lambda (\phi^2 - \eta^2) \phi, \quad (9)$$

where $\partial_z^2 \phi \equiv d^2\phi/dz^2$, $\phi = \phi(\tilde{z})$ with $\tilde{z} = z/\sqrt{1 - k^{11}}$. We observe that the dimensionless factor $\sqrt{1 - k^{11}}$ renormalizes the propagation velocity of the scalar mode with respect to the Fermion maximum speed, namely

$$\frac{v_\phi}{v_F} = \sqrt{1 - k^{11}}. \quad (10)$$

This trivially breaks the covariance of the theory under Lorentz boosts, but applying it to 2D materials, seems rather natural, as the propagation speed of perturbations in the lattice is not required to be the same as the one

for electrons, which in the massless case, corresponds to the Fermi velocity, that for graphene is $v_F \sim c/300$.

An analytic solution of the above nonlinear equation, which interpolates between the different boundary conditions, is the so-called kink. In this case, follows that

$$\phi(z) = \eta \tanh \left[\frac{\alpha_0(z - z_0)}{2} \right], \quad (11)$$

where z_0 is a constant of integration, it can be viewed as specifying the position of the kink. For simplicity, and without loss of generality, we can choose a localized kink centred about $z_0 = 0$, which takes ϕ from $-\eta$ at $z = -\infty$ to η at $z = \infty$. The size of the kink is controlled by:

$$\alpha_0 \equiv \sqrt{2\lambda\eta}/\sqrt{1 - k^{11}}. \quad (12)$$

Note that by varying the speed of the scalar mode by the LV term in the Lagrangian the size of the wall can be tuned.

Now, from Eq. (1), we have the following Dirac equation in the kink background

$$(i\gamma^\mu \partial_\mu - a_\mu \gamma^\mu - i b_\mu \gamma_5 \gamma^\mu - g\phi) \psi = 0, \quad (13)$$

where ϕ is the kink solution given by the Eq. (11) written in terms of the z variable.

From now on, we will solve explicitly the Eq. (13). At this point, it is important to highlight that we will only be interested in determining the bound states. Then, as we are working with two spatial dimensions, the fermions are described by two-component spinors, which we will write as

$$\psi(y, z; t) = \frac{e^{i(\omega y - Et)}}{\sqrt{2}} \begin{bmatrix} \beta_+(z) - \beta_-(z) \\ \beta_+(z) + \beta_-(z) \end{bmatrix}. \quad (14)$$

Therefore, using the above representation into Eq. (13), and after some straightforward manipulations, we can find the following coupled pair of first order differential equations

$$\partial_z \beta_+ + g\phi \beta_+ = -(E + \omega) \beta_-, \quad (15)$$

$$\partial_z \beta_- - g\phi \beta_- = (E - \omega) \beta_+, \quad (16)$$

From now, we will turn our attention concerning the problem of how proceed to decouple the equations (15) and (16). In this case, our goal will be to reduce the differential equations in Schrödinger-like equations, which can be used with advantage in order to understand the essential features of the quantum mechanics of system under analysis. Then, after the substitution we obtain the corresponding second order differential equations

$$-\partial_z^2 \beta_+ + V_+(\phi) \beta_+ = \varepsilon^2 \beta_+, \quad (17)$$

$$-\partial_z^2 \beta_- + V_-(\phi) \beta_- = \varepsilon^2 \beta_-. \quad (18)$$

where we are using the corresponding definitions

$$V_\pm(\phi) \equiv g \left[(g\phi^2 \mp \partial_z \phi) \right]. \quad (19)$$

and

$$\varepsilon^2 \equiv E^2 - \omega^2. \quad (20)$$

Moreover, we can note that Eq. (17) and Eq. (18) are one-dimensional Schrödinger-like equations with potential energy given by $V_\pm[\phi(z)]$, and where both solutions has the same eigenvalue ε^2 .

In the next section, we will calculate both a zero mode and a fermionic bound state on the background of kink given by Eq. (11), with momentum along y , transverse to the direction of action of the trapping potential.

III. DISCRETE FERMION SPECTRUM

In this section, we find the fermion bound states by solving the Schrödinger equation on the background of the kink from the ϕ^4 theory given by Eq. (11). In this case, we follow closely the approach developed by Chu and Vachaspati⁴⁶. For the clarity of the presentation and to define our notation, we repeat the essential steps of that work for the 2+1 case, including the Lorentz symmetry breaking terms of the model.

To begin, we rewrite the potentials $V_\pm(\phi)$ using the kink solution Eq. (11). In this case, we get

$$V_\pm(z) = G^2 - G(G \pm \alpha_0) \text{sech}^2(\alpha_0 z / (\hbar v_F)), \quad (21)$$

where $G = g\eta$ and α_0 is given by Eq. (12). The $\hbar v_F$ factor gives z in units of distance. Next, one needs to calibrate the model parameters to a real situation, as we explain in the following.

In a recent bilayer graphene experiment, it was obtained the images of conducting channels driven by topological states³⁶. The domain wall was created by deformations of one of the layers. The observed conducting channels correspond to states localized at the edges of the domain wall. This experimental configuration leads to the formation of a topological zero mode states which is localized at the border of the domain wall. Naively we can expect the destruction of the peak at the center of the zero mode, as the potential created by the topological deformation for this experimental set up, should be deformed at the middle of the domain wall to include a small barrier at the center, which can imply a double humped state. Of course this effect is not included in our analytical model of the kink, as the effective potential is symmetrical and has the deep at the center of the kink.

Nevertheless the first excited shows the general characteristic peaks at the edges of the domain wall, and due to that we set the parameters of the model to reproduce the relative distance between the two maximum of the first excited state to the observed separation of the conducting channels of 8 nm. We obtain a kink parameter of $\alpha_0 = 20$ meV and $G = 500$ meV. As we are going to see the deep at the minimum of the excited state probability density is controlled by the ratio G/α_0 which should be

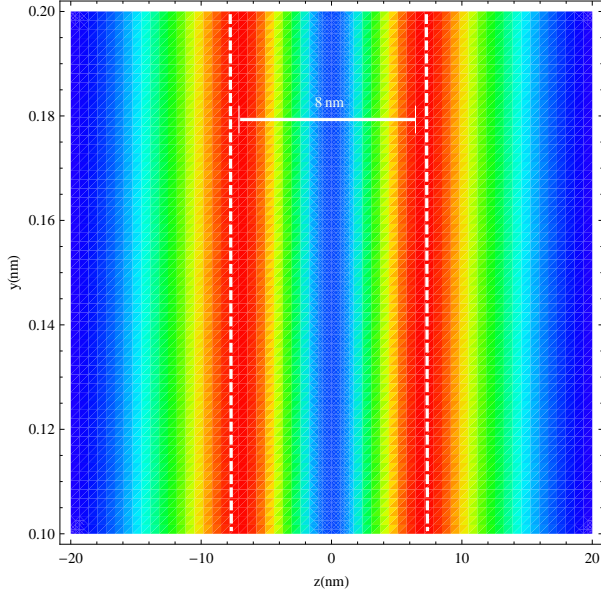


FIG. 1: Charge carrier density distribution corresponding to the first excited state given in Fig. 5.

at least about ~ 10 . To illustrate our choice of parameters, in Fig. 1 we anticipate our results for the charge carrier density of the first excited trapped state, where it is clearly seen the separation of 8 nm between the peaks, and they are located at edge of the domain wall.

We will explore different cases of

$$\alpha_0 = 1 \text{ meV} [v_\phi/v_F]^{-1}, \quad (22)$$

to check the effect of breaking the Lorentz invariance, reminding that the Fermi velocity for the electron is $v_F = c/300$ in graphene.

We should emphasize that the kink in the present topological model, is much simpler than the alluded experimental set up. There are other interesting topological models of superposition of kinks^{73–75}, which could generate a potential closer to the experimental set up, however it is not yet known the analytical solutions of the trapped fermionic modes in these non-trivial kink backgrounds.

It is worth noting that for values of $G > 0$ the potential $V_+(z)$ has the asymptotic maximum of $\lim_{z \rightarrow \pm\infty} V(z) = \eta^2 g^2$, and minimum value of $-G\alpha_0$ at $z = 0$. As it is well known from quantum mechanics in one-dimension, a time-independent attractive potential that tends to zero asymptotically will have at least one bound state. In addition, the Schrödinger-like equation derived for the upper component, has a particular combination of the kink and its derivative, which gives a zero mode³⁷. In general grounds, the zero mode solution of the Dirac equation for a scalar domain wall presents a zero mode (see e.g.⁷²), and was theoretically discovered in the graphene layer near the wall in³⁰. Later on, in Ref.³¹ the zero mode solution was found for the Dirac electron for strained graphene nanoribbons in a soliton trap.

Therefore, it is guaranteed that $V_+(z)$ has at least one

bound state for every g , which is the zero mode. Moreover, since $V_+(z)$ gets deeper with increasing g , there are more and more bound states that appear with larger values of g ⁴⁶. The domain wall created by a kink in 2D materials can present a rich spectrum near the wall driven by the effective potentials $V_\pm(z)$, illustrated in Fig. 2. In addition, the Lorentz violating term drives the potentials by changing the relative speed of the scalar particle to the Fermi velocity Eq. (10) allowing to dial the spectrum with v_ϕ/v_F . We observe in the upper panel of Fig. 2 that the increase of v_ϕ/v_F turns $V_+(z)$ shallow but wider, which indeed increases the number of excited states, as can be seen in $V_-(z)$ in the lower panel of the figure, which becomes deeper and wider allowing more states. We are going to detail analytically such properties of the spectrum.

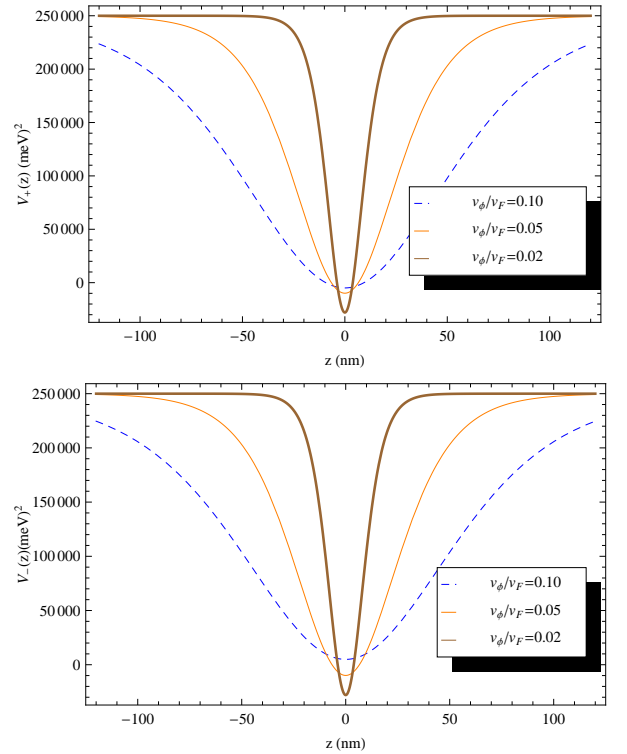


FIG. 2: Effective potentials $V_+(z)$ (upper frame) and $V_-(z)$ (lower frame) obtained with $\sqrt{2\lambda}\eta = 1$ meV, $G = 500$ meV and $\alpha_0 = 1 \text{ meV} [v_\phi/v_F]^{-1}$, for different ratios v_ϕ/v_F of 0.10 (dashed line), 0.05 (thin solid line) and 0.02 (thick solid line).

In order to solve the Dirac equation, we need a non-trivial bound state of the β_- Schrödinger-like equation which has the same energy eigenvalue as for β_+ . Only then β_\pm will solve the first order equations, Eq. (16), except if $\varepsilon = 0$ and for that we can take $\beta_- = 0$. For $0 < g \leq 1$, V_- is in the shape of a potential barrier and clearly has no bound states. This shows that for $0 < g \leq 1$, the only possible bound state is with $\varepsilon = 0$ and $\beta_- = 0$; and the zero mode solution is

$$\beta_+(z) \equiv \beta_{zm}(z) = \text{sech}^{\vartheta_0}(\alpha_0 z / (\hbar v_F)), \quad (23)$$

where $\vartheta_0 = G/\alpha_0$. This zero mode solution near the wall matches the one found in³⁰. This state corresponds to a massless particle moving in the transverse direction, y , with momentum w , and total energy E , as well.

Now, since that there are more bound states for $g > 1$, we will begin our search for these bound states. On the other hand, let us now carry out the quantitative calculation of the stationary states $\beta_{\pm}(z)$, for do this we write

$$\beta_{\pm}(z) = \mathcal{N}_{\pm} \text{sech}^{\vartheta}(\alpha_0 z / (\hbar v_F)) F_{\pm}(z), \quad (24)$$

where $\vartheta \equiv (\sqrt{G^2 - \varepsilon^2})/\alpha_0$. Then, substituting the Eq. (24) into Eqs. (17) and (18), we obtain

$$\begin{aligned} & \partial_z^2 F_+ + 2\alpha_0 \vartheta \tanh(\alpha_0 z / (\hbar v_F)) \partial_z F_+ \\ & + [\alpha_0^2 \vartheta(1 + \vartheta) - G(G + \alpha_0)] \text{sech}^2(\alpha_0 z / (\hbar v_F)) F_+(z) = 0, \end{aligned} \quad (25)$$

$$\begin{aligned} & \partial_z^2 F_- + 2\alpha_0 \vartheta \tanh(\alpha_0 z / (\hbar v_F)) \partial_z F_- \\ & + [\alpha_0^2 \vartheta(1 + \vartheta) - G(G - \alpha_0)] \text{sech}^2(\alpha_0 z / (\hbar v_F)) F_-(z) = 0. \end{aligned} \quad (26)$$

According to⁴⁶, by the variable transformation

$$u = \frac{1}{2} [1 - \tanh(\alpha_0 z / (\hbar v_F))], \quad (27)$$

the equations (25) and (26), becomes

$$\begin{aligned} & u(u-1) \partial_u^2 F_+(u) + (\vartheta+1)(2u-1) \partial_u F_+(u) + \\ & [\vartheta(\vartheta+1) - G(G+\alpha_0)/\alpha_0^2] F_{\pm}(u) = 0, \end{aligned} \quad (28)$$

$$\begin{aligned} & u(u-1) \partial_u^2 F_-(u) + (\vartheta+1)(2u-1) \partial_u F_-(u) + \\ & [\vartheta(\vartheta+1) - G(G-\alpha_0)/\alpha_0^2] F_-(u) = 0, \end{aligned} \quad (29)$$

As we can see, the above equations are the so-called hypergeometric equations, which has the following solutions

$$F_+(u) = \mathcal{N}_+^{(1)} \mathcal{F}[A_+, B_+; C_+; u] \quad (30)$$

$$+ \mathcal{N}_+^{(2)} \mathcal{F}[A_+ + 1 - C_+, B_+ + 1 - C_+; 2 - C_+; u],$$

$$F_-(u) = \mathcal{N}_-^{(1)} \mathcal{F}[A_-, B_-; C_-; u] \quad (31)$$

$$+ \mathcal{N}_-^{(2)} \mathcal{F}[A_- + 1 - C_-, B_- + 1 - C_-; 2 - C_-; u],$$

where the arguments of the hypergeometric function are defined as

$$A_{\pm} \equiv \vartheta_{\pm} + \frac{1}{2} \mp \frac{1}{2} - \frac{G}{\alpha_0}, \quad (32)$$

$$B_{\pm} \equiv \vartheta_{\pm} + \frac{1}{2} \pm \frac{1}{2} + \frac{G}{\alpha_0}, \quad (33)$$

$$C_{\pm} \equiv \vartheta_{\pm} + 1. \quad (34)$$

Therefore, we can write the solutions for $\beta_{\pm}(z)$ in the following form

$$\begin{aligned} \beta_{\pm}(z) &= \mathcal{N}_{\pm}^{(1)} \text{sech}^{\vartheta}(\alpha_0 z / (\hbar v_F)) \mathcal{F}[A_{\pm}, B_{\pm}; C_{\pm}; u] \quad (35) \\ &+ \mathcal{N}_{\pm}^{(2)} e^{\alpha_0 \vartheta z} \mathcal{F}[A_{\pm} - C_{\pm} + 1, B_{\pm} - C_{\pm} + 1; 2 - C_{\pm}; u]. \end{aligned}$$

As shown in⁴⁶, for reason of normalizability, it is necessary to impose that $\mathcal{N}_{\pm}^{(2)} = 0$. Thus, the equation (35) becomes

$$\beta_{\pm}(z) = \mathcal{N}_{\pm}^{(1)} \text{sech}^{\vartheta}(\alpha_0 z / (\hbar v_F)) \mathcal{F}[A_{\pm}, B_{\pm}; C_{\pm}; u]. \quad (36)$$

In addition, we also have the condition

$$\vartheta_n^{\pm} - \frac{G}{\alpha_0} + \frac{1}{2} \mp \frac{1}{2} = -n_{\pm} \in \mathbb{Z}^-. \quad (37)$$

Therefore, after straightforwardly mathematical manipulations, we obtain the energy spectrum

$$\begin{aligned} E_{n-} &= \pm \sqrt{(\hbar\omega)^2 + \alpha_0(n_- + 1)[2G - \alpha_0(n_- + 1)]}, \\ E_{n+} &= \pm \sqrt{(\hbar\omega)^2 + n_+ \alpha_0(2G - \alpha_0 n_+)}. \end{aligned} \quad (38)$$

At this point, it is important to remark that the energy eigenvalues coincide $E_{n+} = E_{n-} \equiv E_n$, which implies in the consistence condition $n_+ - n_- = 1$. Moreover, the normalizability requires $\vartheta_n^+ > 0$, as a consequence we have the constraint

$$1 \leq n_+ < 2G/\alpha_0. \quad (39)$$

The consistence condition for the quantum numbers leads to $\vartheta_n^{\pm} \equiv \vartheta_n$, where $n \equiv n_+$. Just to remind the zero mode is indexed with $n = 0$.

Our solution reduces to the ones found in⁴⁶, when $\alpha_0 \rightarrow 1$, namely the LV term of the scalar field in the Lagrangian vanishes. Note that as have shown the zero mode still survives, independently of this LV interaction term. It builds a zero gap band, as already found in previous works³⁰ and³¹.

IV. DISCUSSION

As we have already discussed, the motivation for the choice of the parameters comes from the experimental work³⁶, where they found by imaging the confined states that the associated conducting channels are mainly located close to the two edges of the domain wall. In that experiment the distance between the two peaks is about 8 nm. In our model the zero mode is peaked at the center of the domain wall, while the first excited state is concentrated at the edges of the domain wall.

A. Spectrum

In order to give some concrete scales of the spectrum, we find the gap Δ between the valence and conducting bands belonging to the first excited state in the trap potential obtained with $n = n_+ = 1$ and $\omega = 0$ in Eq. (38):

$$\Delta = 2\sqrt{\alpha_0(2G - \alpha_0)}, \quad (40)$$

with $\alpha_0 = 20$ meV and $G = 500$ meV, one gets $\Delta = 239$ meV, which is quite large when compared to the value of 80 meV from³⁶. This difference comes from the description of potential in the experimental situation, where one expects to have a wider potential with a barrier in the middle and therefore the level position can be shifted down.

The spectrum for these parameters is shown in Fig. 3. The dispersion relation for the zero mode and the first 38 excited states are presented. The chosen parameters leads to $n_{max} = 50$ from Eq. (39), giving a large number of conducting channels, concentrated at the edges of the kink.

We observe that the quantity $m_n^{\text{eff}} \equiv \sqrt{n\alpha_0(2G - \alpha_0 n)}$ can be interpreted as an effective mass for each of the excited trapped states, which can be written in terms of the gap as:

$$m_n^{\text{eff}} = \sqrt{n \left(\frac{\Delta^2}{4} - \alpha_0^2(n-1) \right)}. \quad (41)$$

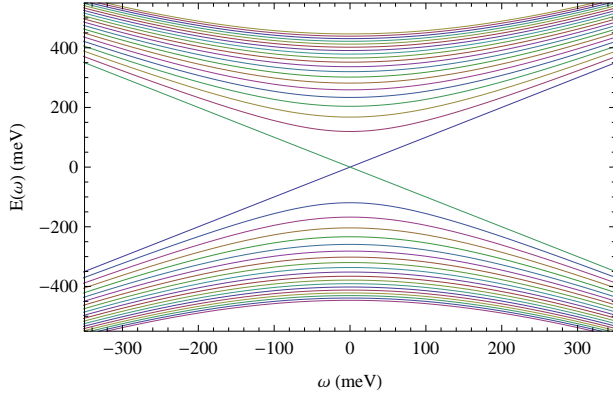


FIG. 3: Band structure for the domain wall obtained with $G = 500$ meV and $\alpha_0 = 20$ meV for the first 39 states, including the zero mode. In this situation the number of states is 101 from $n_{max} = 50$ as follows from Eq. (39).

B. Charge carrier density distribution

On the kink background the wave function of the n -th fermionic state, $\psi_n(y, z; t)$, trapped by the wall, for positive and negative energies, including the zero mode solutions are built from Eqs. (14), (23) and (36).

The zero mode eigenstate of the Dirac Hamiltonian trapped by the soliton is:

$$\psi_0(y, z; t) = N_0 e^{i\omega(y/v_F - t)} \text{sech}^{\vartheta_0} \left(\frac{\alpha_0}{\hbar v_F} z \right) \begin{bmatrix} 1 \\ 1 \end{bmatrix}, \quad (42)$$

which is the solution already found and thoroughly discussed in³¹, apart the LV effect. We have to observe that the zero-mode state in the layer corresponds to the

solution of the one dimensional Dirac equation with a "massless" fermion, as the dispersion relation is $E = \hbar\omega$. In addition the spinor state is an eigenstate of $\gamma^0\gamma^2$. The trapping potential gives a width to the charge distribution along the z direction, as carried the sech term.

The LV term in the scalar field Lagrangian changes only the velocity of the scalar particle ($v_\phi/v_F = \sqrt{1 - k^{11}}$), and in the zero mode solution it only modifies the α_0 and the net effect is to broaden or shrink the wave function, as one sees in Fig. 4 for v_ϕ/v_F equals to 0.1, 0.05 and 0.02; as the velocity ratio becomes larger wider is the state density, as the effective potential also becomes wider as shown in Fig. 2. That comes because the value of α_0 according to Eq. (22), is inversely proportional to v_ϕ/v_F , and α_0 larger/smaller implies in confining potentials narrower/wider.

We have shown results for small values of the velocity ratio and of course could be enhanced by changing more drastically the ratio. This effect could be useful to dial the width of the charge density in the fermion zero mode state in the solitonic trap by modifying the properties of the collective mode propagation, either doping the 2D material, or introducing defects on the lattice, or by a varying strain, etc. This one-dimensional conducting state lives at the middle of the domain wall, while as we are going to show the higher excited states are located mainly close to the edges of the kink.

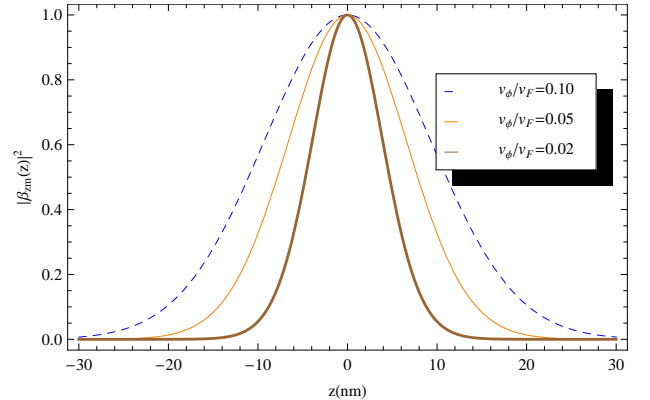


FIG. 4: Density profile of the zero-mode solution with LV term obtained with $G = 500$ meV and $\alpha_0 = 1$ meV $[v_\phi/v_F]^{-1}$, for different ratios v_ϕ/v_F of 0.10 (dashed line), 0.05 (thin solid line) and 0.02 (thick solid line).

The wave function of the excited states in the trapping potential of the kink with $n \geq 1$, are given by:

$$\psi_n(y, z; t) = N_n e^{i(\omega y - E_n t)} \text{sech}^{\vartheta_n} (\alpha_0 z / (\hbar v_F)) \times \begin{bmatrix} -E_n F_+(z) - \alpha_0 n F_-(z) \\ -E_n F_+(z) + \alpha_0 n F_-(z) \end{bmatrix}, \quad (43)$$

where

$$\vartheta_n = \frac{G}{\alpha_0} - n \quad (44)$$

V. CONCLUSIONS

In this work we have investigated the full spectrum of two-dimensional fermion states in a scalar soliton trap with a Lorentz breaking background. It is important to remark that in the context of the novel 2D materials, the Lorentz symmetry should not be strictly valid for a field theory that aims to represent the charge carriers close to the Dirac points and the collective modes of the lattice represented by bosonic fields. The Dirac electron and bosonic fields reflect the non-relativistic dynamics of the electrons and lattice. In that sense, it is natural that the bosonic fields have propagation velocities different from v_F , and the effect of this kind of Lorentz violating effect should be expected when modelling the electronic and lattice excitations in 2D materials, like graphene. Therefore, it is necessary that the Lorentz symmetry breaking should be taken into account in the chosen field theory model. Having that motivation, we have performed an analysis of this particular Lorentz violation effect in a 2D material with a relativistic model of the electrons and fields.

We explore theoretically, the asymmetry between the Fermi and scalar mode velocities, in the wave function of the trapped electrons in a kink background. To accomplish that, we extended the analytical methods developed in the context of 1+1 field theories to study the role of confined fermions to the stability of cosmic strings (see⁴⁶), to explore the effect of the Lorentz symmetry breaking in the charge carrier density of 2D materials in the presence of a domain wall with a kink profile. The width and the depth of the trapping potential from the kink in the presence of the Lorentz violating effect associated with the asymmetry of the Fermi and scalar mode velocities can be manipulated, and is reflected in the band structure and properties of the levels localized along the kink axis and propagating in the transverse direction. The present model provides an analytical form for the rich spectrum enlarging a previous findings of the edge states obtained with domain wall³⁰ and in particular in strained graphene nanoribbon in a chiral gauge theory³¹. In future it will be interesting to generalize our analysis, when transitions between the two valleys are allowed in the field theoretical model, which leads a four dimensional representation of the spinor.

In summary, the bound states solutions of Dirac equation in the kink background are not destroyed by the Lorentz violation due to the different velocities of the Dirac electron and boson modes. One should also expect that theories with gauge fields that aims to describe electronic properties of 2D materials are not necessarily covariant, and Lorentz symmetry breaking effects should be taken into account. We found that by tuning the Lorentz breaking parameter, it is possible to change the density of trapped states and make the associated charge carrier density wider or narrow, which may be of interest in actual applications of 2D materials to electronic devices. Reversely, one could also search the consequences

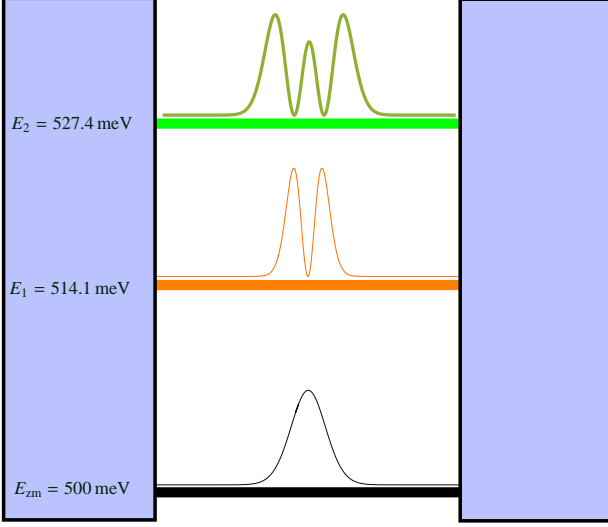


FIG. 5: Probability density of the bound states with positive energy. The electron has a momentum $k_y = \omega$ along the wall, with $\hbar\omega = 500$ meV, $\alpha_0 = 20$ meV and $G = 500$ meV.

$$F_+(z) = \mathcal{F} \left[A_+, B_+; C_+; \frac{1}{2} [1 - \tanh(\alpha_0 z / (\hbar v_F))] \right], \quad (45)$$

$$F_-(z) = \mathcal{F} \left[A_-, B_-; C_-; \frac{1}{2} [1 - \tanh(\alpha_0 z / (\hbar v_F))] \right]. \quad (46)$$

The effect of the Lorentz symmetry breaking term in the scalar field Lagrangian, which corresponds to the scaling of the propagation velocity by α_0^{-1} or $\sqrt{1 - k^2}$, allows to increase/decrease the number of trapped states by increasing/decreasing the speed of the scalar mode in the 2D material, as the condition for the number of states (39) shows for a fixed value of G . Furthermore, the decrease in α_0 increase the density of states.

In Fig. 5, we illustrate the charge carrier density for the lowest states obtained with $\hbar\omega = 500$ meV, $\alpha_0 = 20$ meV and $G = 500$ meV. In this case the density is dominated by $F_+(z)$ due to the energy factor, as seen in Eq.(43). The effect of the LV term expressing the change in the relative speeds of the electron and the scalar quantum, modifies α_0 as shown by Eq. (22), impact both the trapped excited spectrum and in the associated charge carrier densities. For example, by decreasing α_0 from the increase of the scalar mode velocity with respect to v_F , the domain wall becomes softer the charge carrier density swallows.

of Lorentz violation in controlled table top experiments with 2D materials, which could be relevant to understand subtle phenomena in the universe.

Acknowledgments

RACC would like to thank São Paulo Research Foundation (FAPESP), grant 2016/03276-5, for financial sup-

port. WDP, ASD and TF thank to CAPES, CNPq and Fapesp for financial support. RACC gratefully acknowledges José Abdalla Helayel-Neto for discussions at an early stage.

-
- ¹ T. H. R. Skyme, Proc. Roy. Soc. A **262**, 233 (1961).
 - ² A. R. Bishop, T. Schneider, *Solitons and Condensed Matter Physics*, Springer Verlag, Berlin, 1978.
 - ³ E. J. Weinberg, *Classical Solutions in Quantum Field Theory: Solitons and Instantons in High Energy Physics*, Cambridge University Press, Cambridge, England, 2012.
 - ⁴ A. Vilenkin, E. P. S. Shellard, *Cosmic Strings and Other Topological Defects*, Cambridge University, Cambridge, England, 1994.
 - ⁵ R. Rajaraman, *Solitons and Instantons*, North-Holland, Amsterdam, 1982.
 - ⁶ S. J. Orfanidis and R. Wang, Phys. Lett. B **57**, 281 (1975).
 - ⁷ M. J. Duff and C. J. Isham, Nucl. Phys. B **108**, 130 (1976).
 - ⁸ A. Klein, Phys. Rev. D **14**, 558 (1976).
 - ⁹ D. A. Nicole, J. Phys. G **3**, 1463 (1977).
 - ¹⁰ S. Gliga, A. Kákay, R. Hertel, and O. G. Heinonen, Phys. Rev. Lett. **110**, 117205 (2013).
 - ¹¹ M. Kawasaki, K. Saikawa, and T. Sekiguchi, Phys. Rev. D **91**, 065014 (2015).
 - ¹² A. H. Castro Neto, F. Guinea, N. M. R. Peres, K. S. Novoselov and A. K. Geim, Rev. Mod. Phys. **81**, 109 (2009).
 - ¹³ N. M. R. Peres, Rev. Mod. Phys. **82**, 2673 (2010).
 - ¹⁴ M.A.H. Vozmediano, M.I. Katsnelson, F. Guinea, Phys. Rep. **496**, 109 (2010).
 - ¹⁵ P. R. Wallace, Phys. Rev. **71**, 622 (1947).
 - ¹⁶ G. W. Semenoff, Phys. Rev. Lett. **53**, 2449 (1984).
 - ¹⁷ A. J. Chaves, G. D. Lima, W. de Paula, C. E. Cordeiro, A. Delfino, T. Frederico and O. Oliveira, Phys. Rev. B **83**, 153405 (2011).
 - ¹⁸ A. J. Chaves, T. Frederico, O. Oliveira, W. de Paula and M. C. Santos, J. Phys. Condens. Matter **26**, 185301 (2014).
 - ¹⁹ J. K. Pachos, Cont. Phys. **50**, 375 (2009).
 - ²⁰ F. Guinea, B. Horovitz, and P. L. Doussal, Solid St. Commun. **149**, 1140 (2009).
 - ²¹ E. Prada, P. San-Jose, G. León, M. M. Fogler, and F. Guinea, Phys. Rev. B **81**, 161402 (2010).
 - ²² C. Chamon, Phys. Rev. B **62**, 2806 (2000).
 - ²³ R. Jackiw and S.-Y. Pi, Phys. Rev. Lett. **98**, 266402 (2007).
 - ²⁴ C. Chamon, C.-Y. Hou, R. Jackiw, C. Mudry, S.-Y. Pi, and G. Semenoff, Phys. Rev. B **77**, 235431 (2008).
 - ²⁵ O. Oliveira, C. E. Cordeiro, A. Delfino, W. de Paula, T. Frederico, Phys. Rev. B **83**, 155419 (2011).
 - ²⁶ C. Popovici, O. Oliveira, W. de Paula and T. Frederico, Phys. Rev. B **85**, 235424 (2012).
 - ²⁷ E. M. C. Abreu, M. A. de Andrade, L. P. G. de Assis, J. A. Helayel-Neto, A. L. M. A. Nogueira, and R. C. Paschoal, J. High Energy Phys. **05**, 001 (2011).
 - ²⁸ E. M. C. Abreu, M. A. de Andrade, L. P. G. de Assis, J. A. Helayel-Neto, A. L. M. A. Nogueira, and R. C. Paschoal, Ann. Physics. **354**, 618 (2015).
 - ²⁹ C. E. Cordeiro, A. Delfino, T. Frederico, O. Oliveira, W. de Paula, Phys. Rev. B **87**, 045429 (2013).
 - ³⁰ G. W. Semenoff, V. Semenoff, and F. Zhou, Phys. Rev. Lett. **101**, 087204 (2008).
 - ³¹ K. Sasaki, R. Saito, M. S. Dresselhaus, K. Wakabayashi, and T. Enoki, New Jour. Phys. **12**, 103015 (2010).
 - ³² I. Martin, Y.M. Blanter, and A.F. Morpurgo, Phys. Rev. Lett. **100** (2008) 036804.
 - ³³ A. V. Rozhkov, A. O. Sboychakov, A. L. Rakhmanov, and F. Nori, Phys. Rep. **648**, 1 (2016).
 - ³⁴ L. Ju, et al. Nature **520**, 650 (2015).
 - ³⁵ J. Li, K. Wang, K. J. McFaul, Z. Zern, T. Taniguchi, Z. Qiao and J. Zhu, Nature Nanotechnology **11**, 1060 (2016).
 - ³⁶ L.-J. Yin, H. Jiang, J.-B. Qiao and L. He, Nat. Commun. **7**, 11760 (2016).
 - ³⁷ R. Jackiw, C. Rebbi, Phys. Rev. D **13**, 3398(1976).
 - ³⁸ H. J. de Vega, Phys. Rev. D **18**, 2932 (1978).
 - ³⁹ P. Rossi, Nucl. Phys. B **127**, 518 (1977).
 - ⁴⁰ P. D. Vecchia, Nucl. Phys. B **130**, 93 (1977).
 - ⁴¹ R. Jackiw and J. R. Schrieffer, Nucl. Phys. B **190**, 253 (1981).
 - ⁴² I. Romanovsky, C. Yannouleas, and U. Landman, Phys. Rev. B **87**, 165431 (2013).
 - ⁴³ M. Eto, Y. Hirono, M. Nitta, and S. Yasui, PTEP **2014**, 012D01 (2014).
 - ⁴⁴ V. R. Khalilove, Eur. Phys. J. C **74**, 2708 (2014).
 - ⁴⁵ S. Sahoo, Z. Zhang, and J. C. Y. Teo, Phys. Rev. B **94**, 165142 (2016).
 - ⁴⁶ Y. -Z. Chu and T. Vachaspati, Phys. Rev. D **77**, 025006 (2008).
 - ⁴⁷ R. L. Davis, Phys. Rev. D **38**, 3722 (1988).
 - ⁴⁸ A. de Souza Dutra and R. A. C. Correa, Phys. Lett. B **693**, 188 (2010).
 - ⁴⁹ V. A. Kosteletsky and S. Samuel, Phys. Rev. Lett. **63**, 224 (1989).
 - ⁵⁰ V. A. Kosteletsky and N. Hussell, Rev. Mod. Phys. **83**, 11 (2011).
 - ⁵¹ C. M. Cantanhede, R. Casana, M. M. Ferreira, Jr., and E. da Hora, Phys. Rev. D **86**, 065011 (2012).
 - ⁵² R. Casana, M. M. Ferreira, Jr., E. da Hora, and C. Miller, Phys. Lett. B **718**, 620 (2012).
 - ⁵³ R. Casana, M. M. Ferreira, Jr., and E. da Hora, Phys. Rev. D **86**, 085034 (2012).
 - ⁵⁴ R. Casana, M. M. Ferreira, Jr., E. da Hora, and A. B. F. Neves, Eur. Phys. J. C **74**, 3064 (2014).
 - ⁵⁵ R. Casana, M. M. Ferreira, Jr., E. da Hora, and C. dos Santos, Adv. High Energy Phys. **2014**, 210929 (2014).
 - ⁵⁶ C. H. C. Villalobos, J. M. Hoff da Silva, M. B. Hott, and H. Belich, Eur. Phys. J. C **74**, 2799 (2014).

- ⁵⁷ R. Casana, C. F. Farias, and M. M. Ferreira, Jr., Phys. Rev. D **92**, 125024 (2015).
- ⁵⁸ D. Bazeia and R. Menezes, Phys. Rev. D **73**, 065015 (2006).
- ⁵⁹ D. Bazeia, M. M. Ferreira, Jr., A. R. Gomes, and R. Menezes, Physica D **239**, 942 (2010).
- ⁶⁰ A. de Souza Dutra, M. Hott, and F. A. Barone, Phys. Rev. D **74**, 085030 (2006).
- ⁶¹ B. Agostini *et. al.*, Phys. Lett. B **708**, 212 (2012).
- ⁶² A. de Souza Dutra and R. A. C. Correa, Phys. Rev. D **83**, 105007 (2011).
- ⁶³ R. A. C. Correa, R. da Rocha, and A. de Souza Dutra, Ann. Physics **359**, 198 (2015).
- ⁶⁴ R. F. Dashen, B. Hasslacher, and A. Neveu, Phys. Rev. D **10**, 4130 (1974).
- ⁶⁵ A. M. Polyakov, JETP Lett. **20**, 194 (1974).
- ⁶⁶ M. A. Anacleto, F.A. Brito, and E. Passos, Phys. Lett. B **694**, 149 (2011).
- ⁶⁷ M. A. Anacleto, F.A. Brito, and E. Passos, Phys. Lett. B **703**, 609 (2011).
- ⁶⁸ R. A. C. Correa and A. de Souza Dutra, Adv. High Energy Phys. **2014**, 673716 (2014).
- ⁶⁹ R. Jackiw, P. Rossi, Nucl. Phys. B **190**, 681(1981).
- ⁷⁰ R. Jackiw, C. Rebbi, Phys. Rev. D **13**, 3398(1976).
- ⁷¹ E.C.G. Sudarshan, U.A. Yajnik, Phys. Rev. D **33**, 1830(1986).
- ⁷² T. Vachaspati, "Kinks and Domain Walls: An Introduction to Classical and Quantum Solitons", Cambridge University Press, 2006.
- ⁷³ D. Bazeia and F. A. Brito, Phys. Rev. D **61**, 105019 (2000).
- ⁷⁴ A. de Souza Dutra, Phys. Lett. B **626**, 249 (2005).
- ⁷⁵ R. A. C. Correa, A. de Souza Dutra, and M. B. Hott, Class. Quant. Grav. **28**, 155012 (2011).